DOI: https://doi.org/10.57233/ijsgs.v10i2.672 ISSNp: 2488-9229; ISSNe: 3027-1118

IJSGS FUGUSAU VOL10 (2) WEBSITE: https://fugus-

INTERNATIONAL JOURNAL OF SCIENCE FOR GLOBAL SUSTAINABILITY
(A PUBLICATION OF FACULTY OF SCIENCE, FEDERAL UNIVERSITY GUSAU, NIGERIA)

Mixed Convection Flow of a Magnetized Nanofluid with Viscous Dissipation in an Oscillatory System

Emmanuel Omokhuale[1], Jamilu Abubakar[2] and Godwin Ojemeri[3*]

[1]Department of Mathematics, Faculty of Sciences, Federal University Gusau, P. M. B. 1001, Zamfara State.
[2]Department of Mathematics, Faculty of Physical and Computing Sciences, Usmanu Danfodiyo University, P. M. B. 2346, Sokoto State.
[3]Department of Mathematics, College of Sciences, Federal University of Agriculture Zuru, P. M. B. 28, Kebbi State.

***Corresponding Author's Email**: emmanuelomokhuale@gmail.com

Received on: April, 2024 **Revised and Accepted on:** May, 2024 **Published on:** July, 2024

ABSTRACT

This paper attempts to investigate the impacts of mixed convection and viscous dissipation on buoyancy-induced heat and mass transfer of a nanofluid flow through a semi-infinite flat plate in a magnetized oscillating system. The implications of various flow parameters on the velocity, temperature, and concentration distribution of the nanofluid, as well as the skin friction coefficient, Nusselt number, and Sherwood number has been solved semi-analytically using regular perturbation method. The basic governing equations is obtained by employing appropriate transformations techniques which result in high nonlinear coupled differential equations with physical conditions. Different types of nanoparticles are considered, and the salient characteristics of all the embedded parameters on the flow fields have been demonstrated graphically and discussed in detail. It is revealed that, raising the levels of mixed convection and viscous dissipation parameters enhance the fluid velocity respectively. This model has practical applications in the fields of chemical and engineering processes, biomedicine, resonance imaging and so on.

Keywords: Mixed convection, Viscous dissipation, Chemical reaction, Nanofluid, Magnetized Oscillatory flow.

1.0 INTRODUCTION

Recent innovations in nanotechnology have made it much easier to create nanoparticles or nanostructures with higher thermos-physical properties than their bulk counterparts utilizing nuclear or molecular processes. Salah *et al.* (2023) developed Nano fluids by dispersing nanoparticles in a base fluid such as water, oil, or ethylene glycol, to name a few. The study of Nano fluids has witnesses a rise in research activities over the years. Choi (1995) introduced the first nan fluid theory. Several researchers have studied heat and mass transport in MHD Nano fluid flows. To this end, Saleem *et al.* (2024) recently emphasized on the significance of hafnium nanoparticles in hydromagnetic non-Newtonian fluid-particle suspension model through divergent channel with uniform heat source. In a different work, Khedher *et al.* (2024) simulated a novel research to investigate the impacts of thermal and magnetic boundary layer in the presence of viscous dissipation and induced electromagnetic field. Usman and Sanusi (2023) discussed the effects of non-Newtonian Nano fluid flows across a semi-infinite flat plate immersed in a porous medium on heat radiation, Soret, and pressure terms. They took into account the surface temperature and concentration, which are oscillatory in nature due to the presence of various types of nanoparticles. Gbadeyan *et al.* (2020) studied the effect of changing thermal conductivity and viscosity on non-Newtonian Nano fluid flow when convective heating and velocity slip were present. Baoku and Fadare (2018) investigated thermos-diffusion and diffusion-thermo effects on mixed convection hydromagnetic flow in a third grade fluid over a stretching surface in a Darcy forchheimer porous medium and discovered that Soret and Dufour numbers increase as a function of species concentration and thermal boundary thickness. Mabood and Usman (2019) investigated the influence of numerous slips on MHD nanofluid boundary layer flow with heat and mass transfer in a Darcy porous media. They investigated the effect of Darcy number and magnetic field parameters in their work and discovered that increasing the Darcy number and magnetic field parameter leads to increased friction and heat transfer rate.

The study of convection flow of an oscillatory system involving heat and mass transfer saturated with porous medium across various flow channels have been investigated by several scholars. Quite recently, Omokhuale *et al.* (2024) highlighted the consequences of viscous dissipation on a thermally and chemically controlled nanofluid through a boundary layer region in an oscillating system while Usman *et al.* (2024) presented the impact of thermophoresis on magnetized oscillatory system of a buoyancy-induced flow with nanoparticles along a boundary layer regime. In a related paper, Ahmed *et al.* (2024) also investigated the influence of Jeffrey fluid flow with MHD oscillatory system affected by unequal wall temperature along a porous channel. Narayana and Venkateswarlu (2016) studied the consequences of chemical reaction and heat source effects on unsteady MHD free convection heat and mass transfer of a nanofluid flow past a semi-infinite flat plate in a rotating system. The plate is assumed to oscillate in time with steady frequency so that the solutions of the boundary layer are the similar oscillatory type. Sharma *et al.* (2022) emphasized the

analytical study of MHD oscillatory time-dependent free convective viscous incompressible dissipative flow passing through an upstanding channel entrenched with porous medium in the coexistence of heat generation and thermal radiation factors. Falade *et al.* (2017) investigated the implications of suction/injection effects on a time-dependent oscillatory slip flow within an upright vertical channel with unequal wall heating restricted to a transverse magnetic field. Hamza *et al*. (2011) analyzed the impacts of chemical reaction and slip condition on a time-dependent hydromagnetic heat and mass transfer flow across an upstanding channel saturated with porous medium in a rotating system.

Owing to the numerous applications in the chemical and hydrometallurgical industries, the study of heat and mass transfer flow in the presence of chemical reactions has garnered a lot of interest over the years. The two main types of chemical reactions are heterogeneous and homogeneous ones. A chemical reaction is called heterogeneous rather than homogeneous if it occurs at an interface as opposed to in a single phase throughout its volume. In contrast to a homogeneous reaction, which occurs evenly across the entire given phase, a heterogeneous reaction occurs in a confined area or inside the border of a phase. Melting, ceramics and glassware production, catalytic chemical reactors, polymer production, ceramics and glassware production, and the initiation of exothermic or endothermic chemical reactions are just a few of the numerous important applications of heat and mass transfer flows with chemical reactions (Bafakeeh *et al.,* 2022). A number of investigators, conscious of the significance of this type of research, have investigated the hydromagnetic free convection heat and mass transfer flow of a viscous, incompressible, and electrically conducting fluid moving through an upright plate in the presence of a chemical reaction influenced by a variety of flow circumstances. Series of investigations have been carried out by authors on the effect of chemical reactions on various fluid flow regimes. In view of this, Raghunath *et al.* (2022) explored MHD Casson fluid flow across a vertical porous plate under the influence of heat diffusion and chemical reaction in this context. The impact of a chemical reaction on the erratic hydromagnetic natural convective coquette flow in a vertical channel packed with porous materials was studied by Ajibade and Umar (2016). Other studies that looked at how different flow geometries are affected by chemical interactions include the works of Raghunath *et al.* (2021), Raghunath and Obulesu (2022) and Reddy *et al.* (2022).

The primary purpose of this paper is to modify the work of Omokhuale *et al.* (2024) by investigating the impact of mixed convection on a heat and mass controlled magnetized oscillatory flow equipped with Nano elements in the presence of viscous dissipation, porous material and constant pressure gradient. The modeled highly nonlinear partial differential equations in terms of temperature, concentration and velocity are solved semi-analytically using regular perturbation approach. various illustrative graphs have been plotted under the influence of some nanoparticles to showcase the flow pattern of the pertinent embedded parameters dictating the flow. This type of mechanical energy dissipation has a major impact on the fluid's hydrodynamic and thermodynamic behavior, and its attributes has a vast spectrum of applications in the lubrication, food processing, and food preservation industries, as well as in the cooling of electrical appliances and exploration for petroleum products. Additionally, in physics, chemistry, and engineering, the combination of key characteristics such as nanoparticles and heat generating systems has been very useful for enhancing the thermal conductivity of the base fluid and solar collection system.

2.0 STRUCTURE OF THE FLOW

Consider a transient mixed convection flow of a magnetized nanofluid along a semi-infinite porous up-facing plate in an oscillating system with chemical reaction, Soret effect and thermal radiation. It is assumed that there is no applied voltage which implies the absence of an electric field. The flow is assumed to be in the x -direction which is taken along the plate in the upward direction, the Y –axis is normal to it and the z axis along the width of the plate as shown in Figure 1. Also it is assumed that the whole system is rotate with a constant vector Ω about z –axis. Due to semi-infinite plate surface assumption the flow variables are functions of z and time t only. Following Omokhuale *et al.* (2024) and assuming that the fluid is controlled by mixed convection parameter with constant pressure gradient, the partial differential equations governing the flow can be expressed in dimensional form as follow:

DOI: https://doi.org/10.57233/ijsgs.v10i2.672 ISSNp: 2488-9229; ISSNe: 3027-1118
IJSGS FUGUSAU VOL10 (2) WEBSITE: https://fugus-

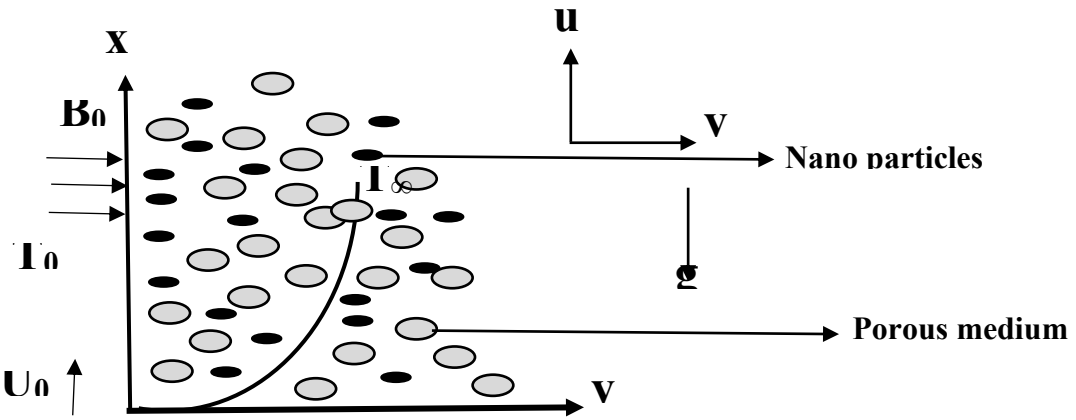

Figure 1: Schematic diagram of the flow domain

Continuity Equation:

$$\frac{\partial w'}{\partial z'} = 0 \tag{1}$$

Momentum Equation:

$$\frac{1}{\rho_{nf}}\left\{\mu_{nf}\frac{\partial^2 u'}{\partial z'^2} + (\rho\beta)_{nf} g\beta(T' - T'_\infty) - \frac{v_f u'}{k} - \frac{\sigma\beta_0^2 u'}{\rho} - \frac{1}{\rho}\frac{\partial P}{\partial z'}\right\} - \frac{\partial u'}{\partial t'} - w'\frac{\partial u'}{\partial z'} + 2\Omega = 0 \tag{2}$$

$$\frac{1}{\rho_{nf}}\left\{\mu_{nf}\frac{\partial^2 v'}{\partial z'^2} - \frac{v_f v'}{k} - \frac{\sigma\beta_0^2 v'}{\rho}\right\} - \frac{\partial v'}{\partial t'} - w'\frac{\partial v'}{\partial z'} - 2\Omega u' = 0 \tag{3}$$

Energy Equation:

$$\alpha_{nf}\frac{\partial^2 T'}{\partial y'^2} - \frac{Q_H}{(\rho C_P)_{nf}}(T' - T'_\infty) + \frac{v}{c_\rho}\left[\left(\frac{\partial U'}{\partial z'}\right)^2\right] - \frac{\partial T'}{\partial t'} - w'\frac{\partial T'}{\partial z'} = 0 \tag{4}$$

Mass Concentration /Diffusion Equation:

$$D_m\frac{\partial^2 c'}{\partial z'^2} + D_L\frac{\partial^2 T'}{\partial z'^2} - R_m(C' - C'_\infty) - \frac{\partial c'}{\partial t'} - w'\frac{\partial c'}{\partial z'} = 0 \tag{5}$$

The appropriate boundary conditions are:

$$u'(z't') = 0, v'(z't') = 0, T(z't') = 0,\ C(z't') = 0\ \ for\ t' \le 0$$
$$u'(z't') = 1 + \frac{\varepsilon}{2}(e^{int} + e^{-int}), v(0,t) = 0, T(0,t') = 1,\ C(0,t') = 1$$
$$u'(\infty,t') \to 0, v'(\infty,t') \to 0, T'(\infty,t') \to 0,\ C'(z't') \to 0\ for\ t \ge 0 \tag{6}$$

The properties of nanofluids are defined as follows:

$$p_{nf} = (1-\emptyset)p_f + \emptyset p_s,\ (\rho C_p)_{nf} = (1-\emptyset)(\rho C_p)_f + \emptyset(\rho C_p)_s$$
$$(\rho\beta)_{nf} = (1-\emptyset)(\rho\beta)_f + \emptyset(\rho\beta)_s,\ \mu_{nf} = \frac{\mu_f}{(1-\emptyset)^{2.5}},\ \alpha_{nf} = \frac{K_{nf}}{(\rho C_p)_{nf}}$$
$$K_{nf} = K_f\left\{\frac{K_s + 2K_f - 2\emptyset(K_f - K_s)}{K_s + 2K_f + 2\emptyset(K_f - K_s)}\right\} \tag{7}$$

where the nondimensional quantities and parameters are:

$$u = \frac{u'}{U_0}, v = \frac{v'}{U_0}, z = \frac{U}{vf}z', t = \left(\frac{vf}{U^2}\right)t', n = \left(\frac{U^2}{vf}\right)n', R = \frac{2\Omega vf}{U^2}, S = \frac{w_0}{U}, Sc = \frac{v}{D_B}, Sr = \frac{D_T(T_W - T_\infty)}{(C_W - C_\infty)T_\infty}, T = \frac{(T - T_\infty)}{(T_W - T_\infty)}, C = \frac{(C - C_\infty)}{(C_W - C_\infty)}, B_r = EcPr, Gr = \frac{g\beta(T'_1 - T_0)x^3}{v^2}, Re = \frac{U_0 x}{v}, \gamma = \frac{1}{\rho}\frac{\partial P}{\partial x}, Da = \frac{k}{h^2}, Ha = \frac{\sigma\beta_0^2 h^2}{\rho v}$$ where

$$Ec = \frac{U_0^2}{c_p(T_w - T_\infty)} \text{ and } \Pr = \frac{\nu}{\alpha_{nf}} \tag{8}$$

substituting eqn (8) into eqns (2-6), we have the following nondimensional equations:

$$\frac{1}{A_1}\frac{\partial^2 u}{\partial z^2} + A_4\frac{Gr}{Re}T - \left(Ha + \frac{1}{Da}\right)u - A_3\left\{\frac{\partial u}{\partial t} + S\frac{\partial u}{\partial z} + Rv\right\} = \gamma \tag{9}$$

$$\frac{1}{A_1}\frac{\partial^2 u}{\partial z^2} - \left(Ha + \frac{1}{Da}\right)v - A_3\left\{\frac{\partial u}{\partial t} + S\frac{\partial u}{\partial z} + Ru\right\} = 0 \tag{10}$$

$$A_5\left\{\frac{\partial T}{\partial t} - S\frac{\partial T}{\partial z}\right\} = \frac{1}{Pr}\left\{A_2\frac{\partial^2 T}{\partial z^2} - QT\right\} + Br\left[\frac{\partial U}{\partial z}\right]^2 \tag{11}$$

DOI: https://doi.org/10.57233/ijsgs.v10i2.672 ISSNp: 2488-9229; ISSNe: 3027-1118
IJSGS FUGUSAU VOL10 (2) WEBSITE: https://fugus-

$$\frac{\partial C}{\partial t} - S\frac{\partial C}{\partial z} = \frac{1}{Sc}\frac{\partial^2 C}{\partial z^2} + Sr\frac{\partial^2 T}{\partial z^2} - KrC \quad (12)$$

where $A_1 = (1-\emptyset)^{2.5}$, $A_2 = \frac{K_{nf}}{K_f}, A_3 = 1 - \emptyset + \emptyset\left(\frac{p_s}{p_f}\right), A_4 = 1 - \emptyset + \emptyset(p\beta)/(p\beta)_f$

$A_5 = 1 - \emptyset + \emptyset(\rho C_p)/(\rho C_p)_f$

The relevant boundary conditions now become:

u(z, t) = 0, v(z, t) = 0, T(z, t)=0, C(z, t)=0 for $t \leq 0$ *any* z

u(0, t)=1+$\frac{\varepsilon}{2}(e^{int} + e^{-int})$, $v(0,t) = 0, T(0,t) = 1, C(0,t) = 1$

$u(\infty, t) \to 0, v(\infty, t) \to 0, T(\infty, t) \to 0, C(\infty, t) \to 0 \; for \; t \geq 0$ (13)

Using eqn (9) the velocity characteristics U_0 is defined as:

$U_0 = \{g\beta_f(T_w - T_\infty)vf\}^{1/3}$

To obtain the desired solutions, we now simplify eqns (9-12) by transforming the fluid velocity into complex form as:

$U(z,t) = u(z,t) + iv(z,t)$ and we get

$$\frac{1}{A_1}\frac{\partial^2 U}{\partial z^2} + A_4\frac{Gr}{Re}T - \left(Ha + \frac{1}{Da}\right)U - A_3\left\{\frac{\partial U}{\partial t} + S\frac{\partial U}{\partial z} + iRU\right\} = \gamma \quad (14)$$

The associated boundary conditions in eqn (13) become:

U(z, t) = 0, T(z, t)=0, C(z, t)=0 for $t \leq 0$ *any* z

U(0, t)=1+$\frac{\varepsilon}{2}(e^{int} + e^{-int})$, $T(0,t) = 1, C(0,t) = 1$

$U(\infty, t) \to 0, v(\infty, t) \to 0, T(\infty, t) \to 0, C(\infty, t) \to 0 \; for \; t \geq 0$ (15)

3.0 SOLUTION PROCEDURE

To find the analytical solutions of the above system of partial differential equations (11), (12) and (14) subject to the boundary conditions (15) in the neighborhood of the plate, we assume that:

$$U(z,t) = U_0(z,t) + \frac{\varepsilon}{2}\{e^{int}U_1\} \quad (16)$$

$$T(z,t) = T_0(z,t) + \frac{\varepsilon}{2}\{e^{int}T_1\} \quad (17)$$

$$C(z,t) = C_0(z,t) + \frac{\varepsilon}{2}\{e^{int}C_1\} \quad (18)$$

Due to the nonlinearity of this resultant governing equations, we further make the following assumptions:

$$\left.\begin{aligned} U_0(z,t) &= U_{00}(z,t) + Br[U_{01}(z,t)] \\ U_1(z,t) &= U_{10}(z,t) + Br[U_{11}(z,t)] \end{aligned}\right\} \quad (19)$$

$$\left.\begin{aligned} T_0(z,t) &= T_{00}(z,t) + Br[T_{01}(z,t)] \\ T_1(z,t) &= T_{10}(z,t) + Br[T_{11}(z,t)] \end{aligned}\right\} \quad (20)$$

$$\left.\begin{aligned} C_0(z,t) &= C_{00}(z,t) + Br[C_{01}(z,t)] \\ C_1(z,t) &= C_{10}(z,t) + Br[C_{11}(z,t)] \end{aligned}\right\} \quad (21)$$

Substituting eqns (19-21) into eqns (11), (12) and (14), and comparing the coefficients of Br^0 and Br^1, after involving the above equations (16-18) into eqns (9-12) and equating the harmonic and non-harmonic terms and neglecting the higher order terms of $O(\varepsilon^2)$, we obtain the following set of equations:

The zeroth order equations are:

Momentum equations

$$\frac{1}{A_1}\frac{\partial^2 U_{00}}{\partial z^2} + A_3 S\frac{\partial U_{00}}{\partial z} - \left(A_3 iR + Ha + \frac{1}{Da}\right)U_{00} + A_4\frac{Gr}{Re}T_{00} = \gamma \quad (22)$$

$$\frac{1}{A_1}\frac{\partial^2 U_{01}}{\partial z^2} + A_3 S\frac{\partial U_{01}}{\partial z} - \left(A_3 iR + Ha + \frac{1}{Da}\right)U_{01} + A_4\frac{Gr}{Re}T_{01} = 0 \quad (23)$$

Energy equations

$$A_2\frac{\partial^2 T_{00}}{\partial z^2} + A_5 SPr\frac{\partial T_{00}}{\partial z} - QT_{00} = 0 \quad (24)$$

$$A_2\frac{\partial^2 T_{01}}{\partial z^2} + A_5 SPr\frac{\partial T_{01}}{\partial z} - QT_{01} = -Pr\left[\frac{\partial U_{00}}{\partial z}\right]^2 \quad (25)$$

Mass flux equations

DOI: https://doi.org/10.57233/ijsgs.v10i2.672 ISSNp: 2488-9229; ISSNe: 3027-1118
IJSGS FUGUSAU VOL10 (2) WEBSITE: https://fugus-

$$\frac{\partial^2 C_{00}}{\partial z^2} + SSc\frac{\partial C_{00}}{\partial z} - ScKrC_{00} = -ScSr\frac{\partial^2 T_{00}}{\partial z^2} \quad (26)$$
$$\frac{\partial^2 C_{01}}{\partial z^2} + SSc\frac{\partial C_{01}}{\partial z} - ScKrC_{01} = -ScSr\frac{\partial^2 T_{01}}{\partial z^2} \quad (27)$$

The first order equations are

Momentum equations

$$\frac{1}{A_1}\frac{\partial^2 U_{10}}{\partial z^2} + A_3 S\frac{\partial U_{10}}{\partial z} - \left(A_3 iR + Ha + \frac{1}{Da}\right)U_{10} + A_4\frac{Gr}{Re}T_{10} = \gamma \quad (28)$$
$$\frac{1}{A_1}\frac{\partial^2 U_{11}}{\partial z^2} + A_3 S\frac{\partial U_{11}}{\partial z} - \left(A_3 iR + Ha + \frac{1}{Da}\right)U_{11} + A_4\frac{Gr}{Re}T_{11} = 0 \quad (29)$$

Energy equations

$$A_2\frac{\partial^2 T_{10}}{\partial z^2} + A_5 SPr\frac{\partial T_{10}}{\partial z} - QT_{10} = 0 \quad (30)$$
$$A_2\frac{\partial^2 T_{11}}{\partial z^2} + A_5 SPr\frac{\partial T_{11}}{\partial z} - QT_{11} = -Pr\left[\frac{\partial U_{10}}{\partial z}\right]^2 \quad (31)$$

Mass flux equations

$$\frac{\partial^2 C_{10}}{\partial z^2} + SSc\frac{\partial C_{10}}{\partial z} - ScKrC_{10} = -ScSr\frac{\partial^2 T_{10}}{\partial z^2} \quad (32)$$
$$\frac{\partial^2 C_{11}}{\partial z^2} + SSc\frac{\partial C_{11}}{\partial z} - ScKrC_{11} = -ScSr\frac{\partial^2 T_{11}}{\partial z^2} \quad (33)$$

The corresponding boundary conditions can simply be written as:

$$U_{00} = U_{01} = U_{10} = U_{11} = 1, T_{00} = T_{01} = T_{10} = T_{11} = 1, C_{00} = C_{01} = C_{10} = C_{11} = 1 \; at \; z = 0$$
$$U_{00} = U_{01} = U_{10} = U_{11} = 0, T_{00} = T_{01} = T_{10} = T_{11} = 0, C_{00} = C_{01} = C_{10} = C_{11} = 0 \; at \; z \to \infty \quad (34)$$

Solving the above equations restricted to the boundary conditions (34), we obtain the expressions for velocity, temperature and concentration as:

$$T_{00} = e^{-c_2 z} \quad (35)$$
$$T_{01} = H_4 e^{-c_4 z} + H_5 e^{-2c_{18} z} + H_6 e^{-c_{18} - c_2 z} + H_7 e^{-2c_2 z} \quad (36)$$
$$T_{10} = e^{-c_6 z} \quad (37)$$
$$T_{11} = H_9 e^{-c_8 z} + H_{10} e^{-2c_{20} z} + H_{11} e^{-c_{20} - c_6 z} + H_{12} e^{-2c_6 z} \quad (38)$$

$$C_{00} = L_2 e^{-c_{10} z} + L_3 e^{-c_2 z} \quad (39)$$
$$C_{01} = L_5 e^{-c_{12} z} + L_6 e^{-c_4 z} + L_7 e^{-2c_{18} z} + L_8 e^{-c_{18} z - c_4 z} + L_9 e^{-2c_2 z} \quad (40)$$
$$C_{10} = L_9 e^{-c_{14} z} + L_{10} e^{-c_6 z} \quad (41)$$
$$C_{11} = L_{14} e^{-c_{16} z} + L e^{-c_8 z} + L_{16} e^{-2c_{20} z} + L_{17} e^{-c_{20} - c_6 z} + L_{18} e^{-2c_6 z} \quad (42)$$

$$U_{00} = E_2 e^{-c_{18} z} + E_3 e^{-c_2 z} \quad (43)$$
$$U_{01} = E_5 e^{-c_{20} z} + E_6 e^{-c_4 z} + E_7 e^{-2c_{18} z} + E_8 e^{-c_{18} z - c_2 z} + E_9 e^{-2c_2 z} \quad (44)$$
$$U_{10} = E_9 e^{-c_{20} z} + E_{10} e^{-c_6 z} \quad (45)$$
$$U_{11} = E_{13} e^{-c_{22} z} + E_{14} e^{-c_8 z} + E_{15} e^{-2c_{20} z} + E_{16} e^{-c_{20} z - c_8 z} + E_{17} e^{-2c_6 z} \quad (46)$$

Recall that,

$$U(z,t) = U_0 + \frac{\varepsilon}{2}\{e^{int} U_1\} \quad (47)$$
$$T(z,t) = T_0 + \frac{\varepsilon}{2}\{e^{int} T_1\} \quad (48)$$
$$C(z,t) = C_0 + \frac{\varepsilon}{2}\{e^{int} C_1\} \quad (49)$$

The physical quantities of engineering interest are also calculated such as skin friction, Nusselt number and Sherwood number coefficients, which have been derived as:

$$\left.\frac{dU}{dz}\right|_{z=0} = -c_{18}E_2 - c_2 E_3 + Br(-c_{20}E_5 - c_4 E_6 - 2c_{18}E_7 - (c_{18} + c_2)E_8 - 2c_2 E) + \frac{\varepsilon}{2}[-c_{20}E_{10} - c_6 E_{11} + Br(-c_{22}E_{13} - c_8 E_{14} - 2c_{20}E_{15} - (c_{20} + c_6)E_{16} - 2c_6 E_{17})]e^{int} \quad (50)$$

$$\left.\frac{dT}{dz}\right|_{z=0} = -c_2 + Br(-c_4 H_4 - 2c_{18}H_5 - (c_{18} + c_2)H_6 + -2c_2 H_7) + \frac{\varepsilon}{2}[-c_6 + Br(-c_8 A_9 - 2c_{20}H_{10} - (c_{20} + c_6)H_{11} + -2c_6 H_{12})]e^{int} \quad (51)$$

DOI: https://doi.org/10.57233/ijsgs.v10i2.672 ISSNp: 2488-9229; ISSNe: 3027-1118
IJSGS FUGUSAU VOL10 (2) WEBSITE: https://fugus-

$$\left.\frac{dC}{dz}\right|_{z=0} = -c_{10}L_2 - c_2L_3 + Br(-c_{12}L_5 - c_4L_6 - 2c_{18}L_7 - (c_{18}+c_2)L_8 - c_4L_9) + \frac{\varepsilon}{2}[-c_{14}L_9 - c_6L_{10} + Br(-c_{16}L_{14} - c_8L_{15} - 2c_{20}L_{16} - (c_{20}+c_6)L_{17} - 2c_6L_{18})]e^{int} \quad (52)$$

The expressions for all constants are provided in the appendix section.

4.0 RESULTS AND DISCUSSION

In this section, we present the results and discussion of the investigation of the impacts of viscous dissipation and permeability on MHD oscillatory heat and mass flow across a porous channel affected by thermal diffusion, chemical reaction and heat absorption. In order to get physical insight into the problem, we have carried out numerical evaluation for non-dimensional velocity, temperature and species concentration, skin-friction, and Nusselt number by assigning some specific values to the embedded parameters dictating the flow for basically two different types of water based nanofluids. For this purpose, Figures 3-11 have been plotted and discussed. Table 1 shows the thermo physical properties of water and the Nano elements Cu, Ai_2O_3 *and* TiO_2. To ascertain the validity and correctness of this present investigation, the graphs for temperature and velocity profiles as shown in Figure 2a and b for Omokhuale *et al.* (2024) and the current study for limiting case when $Br = \gamma = 0$ *and* $Gre = 1$ for fixed values of ε =0.01; R = 0.02 n =10.0; t = 0.1; Ha = 0.5, Da = S = Kr=1; Q=10.0: $\emptyset = 0.15$.

Table 1: Thermo-physical properties

Physical properties	Water	Copper (Cu)	Aluminium Oxide (Al_2O_2)	Titanium oxide (TiO_2)
C_p	4179	385	765	686.2
$\boldsymbol{\rho}$	997.1	8933	3970	4250
K	0.613	400	40	8.9538
$\boldsymbol{\beta \times 10^{-5}}$	21	1.67	0.85	0.9

The comparison demonstrates an excellent relationship. Figures 3 and 4 present the effects of the viscous dissipation parameter Br on the temperature and velocity gradients respectively. With an increase in Br, the temperature of the fluid increases. Equally, an increase in Br results to an increase in the fluid velocity. Higher Brickman numbers mean correspondingly higher degrees of convective heating at the lower channel wall and consequently lead to high temperature and velocity at the lower plate. Figure 5 illustrates the behaviour of mixed convection parameter on velocity profile. It is seen that, mounting level of mixed convection parameter is observed to enhance the fluid flow and this effect is higher in the case cu-water element. The deviations of temperature profiles for different values of heat sink parameter Q is sketched in Figure 6. It is clear that, there is a decrease in the temperature with increase of Q. This is due to the fact that when heat is absorbed, the buoyancy forces decrease which retard the flow rate and thereby give rise to a decrease in the temperature profile. The variations of Darcy porous parameter on the velocity gradient is illustrated in Figure 7. It is depicted from this figure that the action of the Darcy porosity parameter on the velocity nanoparticles gradient. It is perceived from this figure that the velocity fluid accelerates as the porosity parameter is increased. We observe that, with the growth in permeability of the porous medium, the drag force weakens; because of this, velocity gradient of the fluid blows up. Moreover, this makes sense because when a lot of fluid is moved, more viscous energy is made. This causes the fluid boundary wall and thickness to grow, which speeds up the movement of the fluid. Figure 8 shows the influence of magnetic field parameter Ha on the velocity Nanofluid profiles in the boundary layer. Application of magnetic field to an electrically conducting fluid gives rise to a resistive type force called the Lorentz force. This force has the tendency to slow down the motion of the fluid in the boundary layer. Thus the presence of the magnetic field parameter decreases the momentum boundary layers' thickness. Figure 9 shows the effect of chemical reaction (Kr) on concentration profile. Its observed that increase in chemical reaction parameter decreases the concentration profile. The rationale is that as chemical reactions increases, the quantity of solute molecules undergoing them grows, this causes concentration to drop, which in turn reduces the likely-hood of destructive chemical reaction. In other words, the concentration asymptotically decreases from the maximum value 1 to 0 as z →∞. This shows that the concentration field is greatest near the plate surface and least in the outer flow region. The same figure further indicates that there is a steady fall in species concentration due to the effect of chemical reaction. This means that the consumption of chemical species leads to fall in the species concentration field. This clearly agrees with the

DOI: https://doi.org/10.57233/ijsgs.v10i2.672 ISSNp: 2488-9229; ISSNe: 3027-1118

physical laws. Figure 10 demonstrates how the species concentration rises along with the number of Sorets. A rise in the Soret effect, by definition, indicates an increase in molar mass diffusivity. An increase in the increase in concentration is due to molecule mass diffusivity. This shows that the species concentration in the fluid tends to rise as the Soret number rises. The deviations of magnetic number versus suction/injection parameters on the skin friction is displayed in Figure 11. It is evident that increasing the magnetic and suction/injection effects strengthens the skin friction and this effect is higher in the case of Cu-water nano element than Ai_2O_3 *and* TiO_2 nano elements. The implication of Br on the shear stress against suction/injection is exhibited in Figure 12. The exhibition explains that higher Br promotes the frictional force especially at the heated plate. The coefficient of Nusselt number is plotted against Q for different values of Br in Figure 13. It is obvious that the rates of heat transfer increase with rising values of Br. It is also notuced that Cu - water nanofluid has the highest Nusselt number.

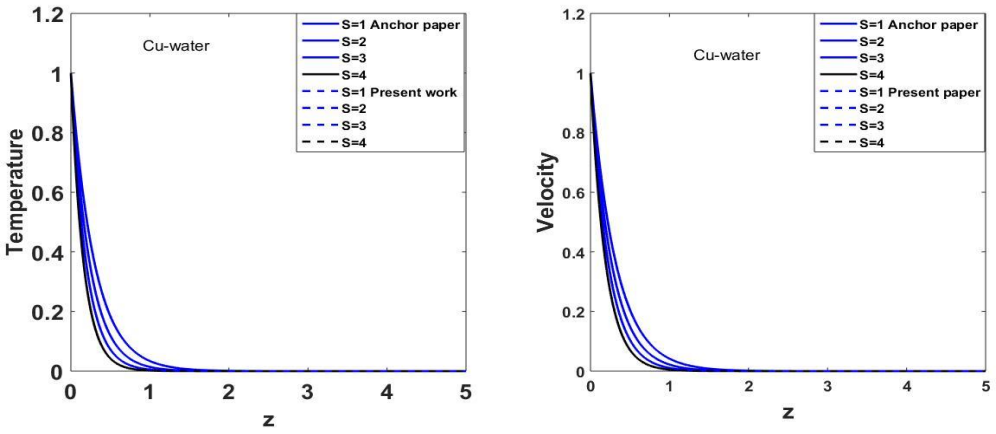

Figure 2: Comparison of Omokhaule *et al.* (2024) with the present work for (a) temperature and (b) velocity gradient

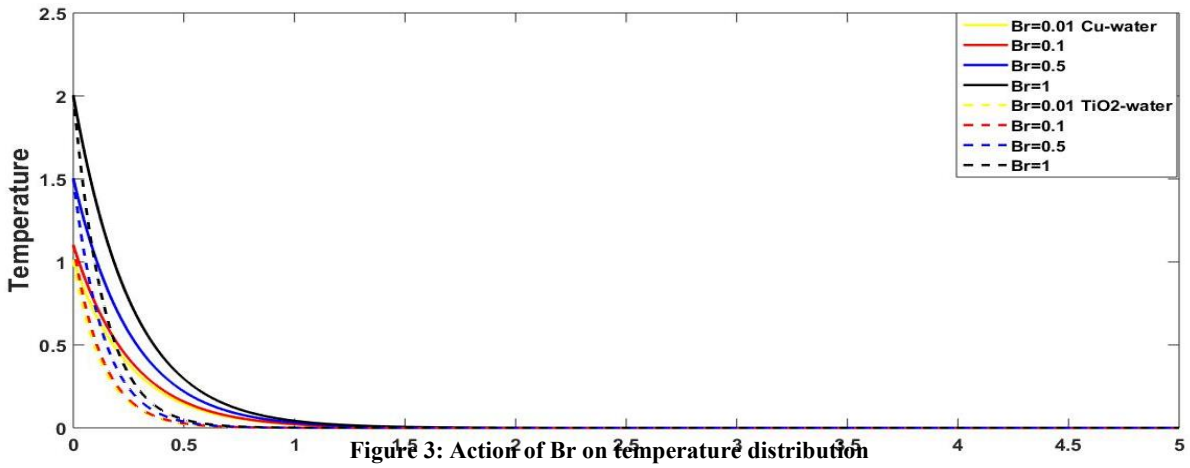

Figure 3: Action of Br on temperature distribution

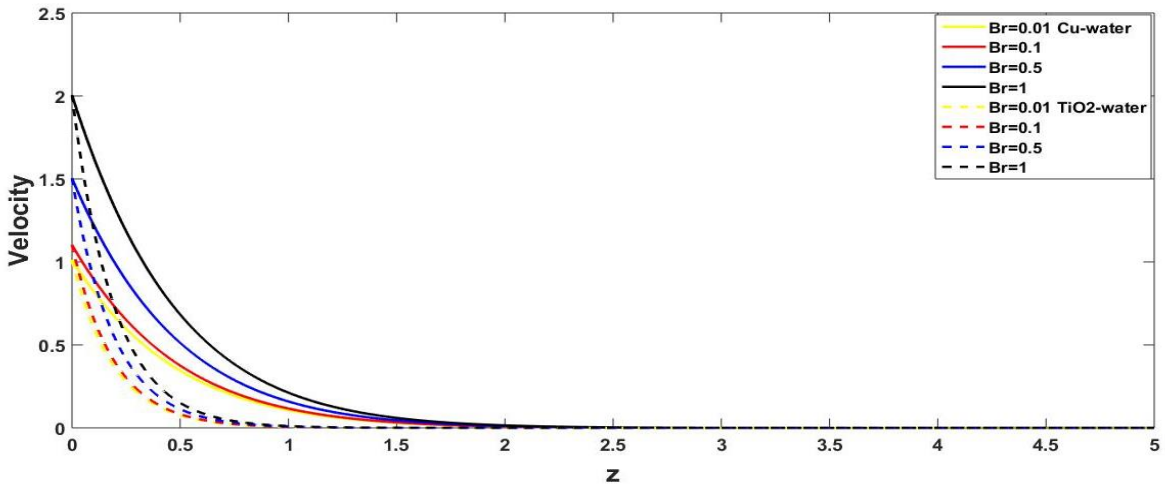

DOI: https://doi.org/10.57233/ijsgs.v10i2.672 ISSNp: 2488-9229; ISSNe: 3027-1118
IJSGS FUGUSAU VOL10 (2) WEBSITE: https://fugus-

Figure 4: Action of Br on Velocity distribution

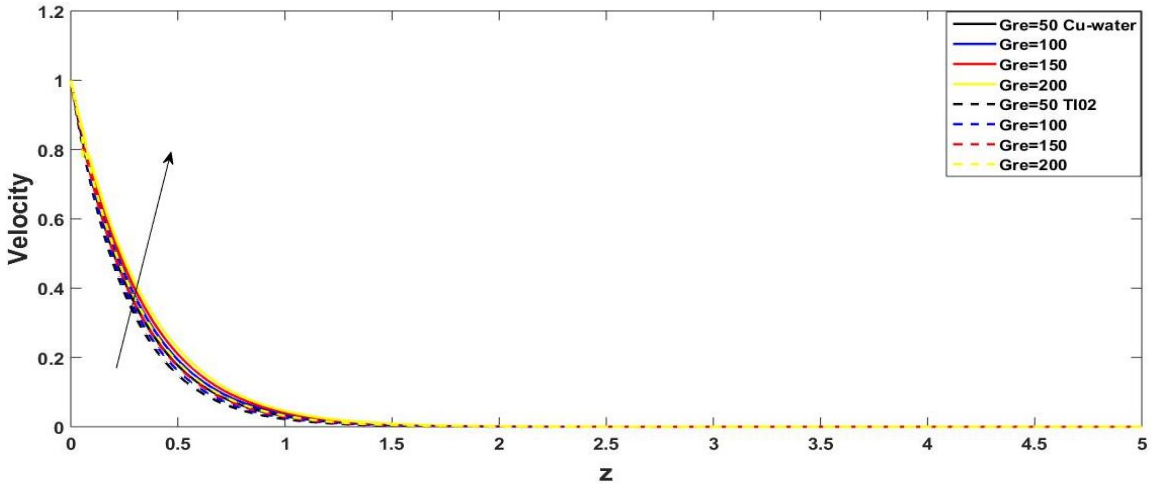

Figure 5: Action of Gre on Velocity distribution

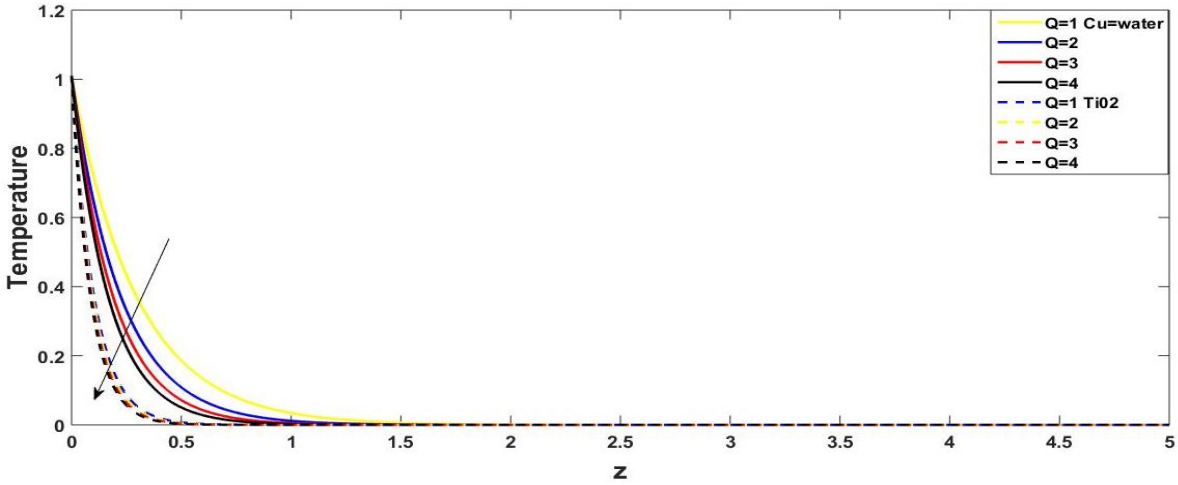

Figure 6: Action of Q on temperature distribution

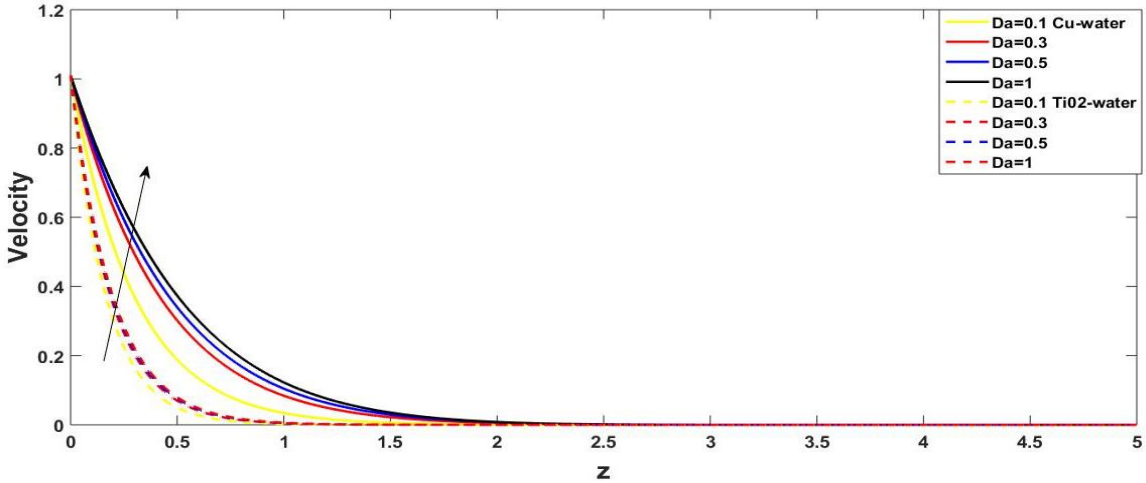

Figure 7: Action of Da on velocity distribution

DOI: https://doi.org/10.57233/ijsgs.v10i2.672 ISSNp: 2488-9229; ISSNe: 3027-1118
IJSGS FUGUSAU VOL10 (2) WEBSITE: https://fugus-

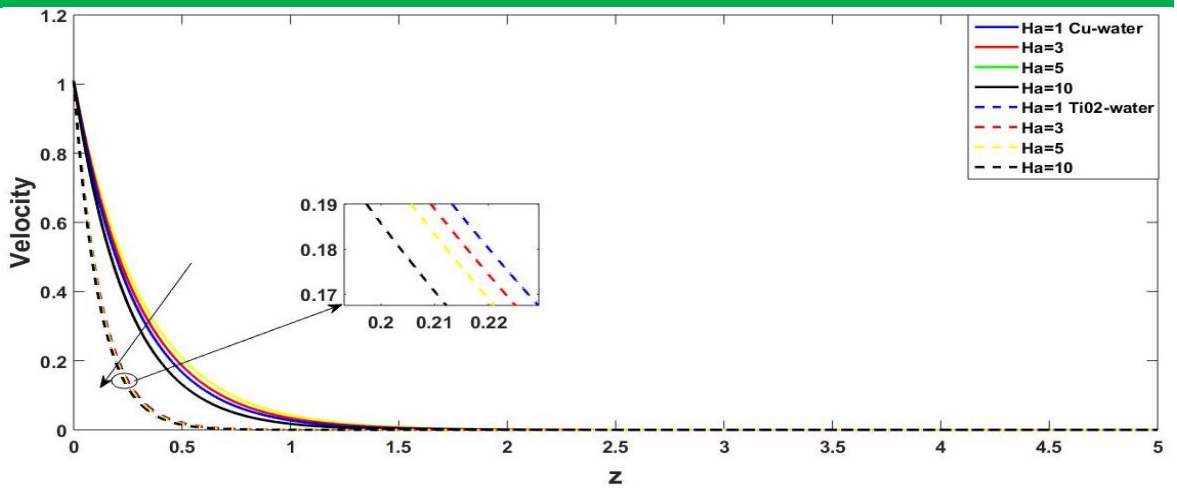

Figure 8: Action of Ha on velocity distribution

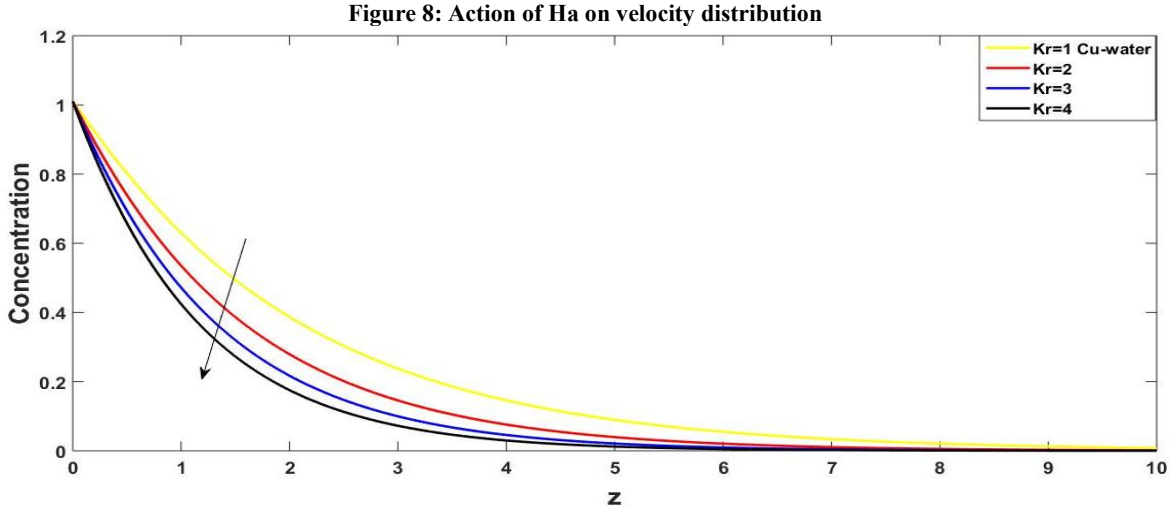

Figure 9: Action of Kr on concentration distribution

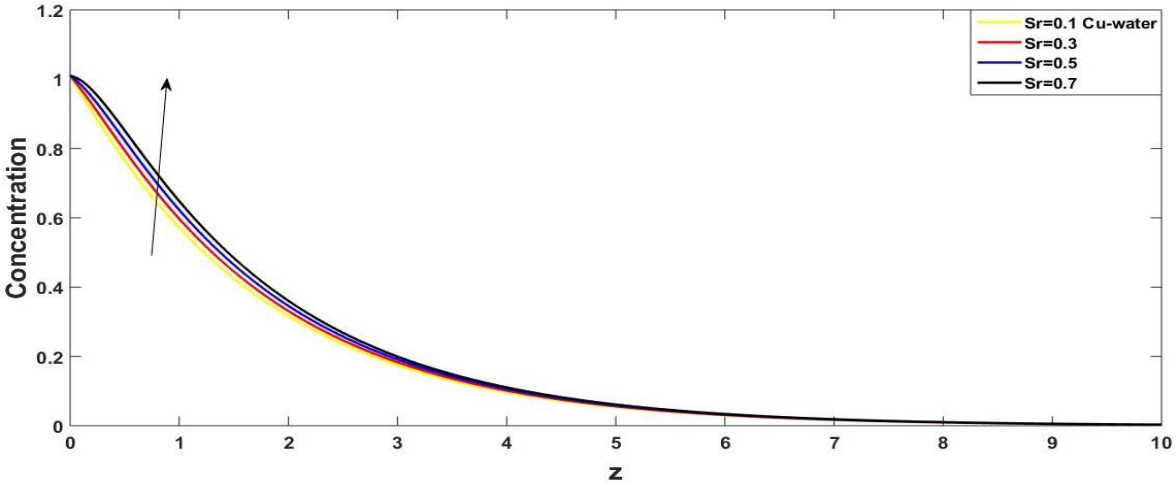

Figure 10: Action of Sr on concentration distribution

DOI: https://doi.org/10.57233/ijsgs.v10i2.672 ISSNp: 2488-9229; ISSNe: 3027-1118
IJSGS FUGUSAU VOL10 (2) WEBSITE: https://fugus-

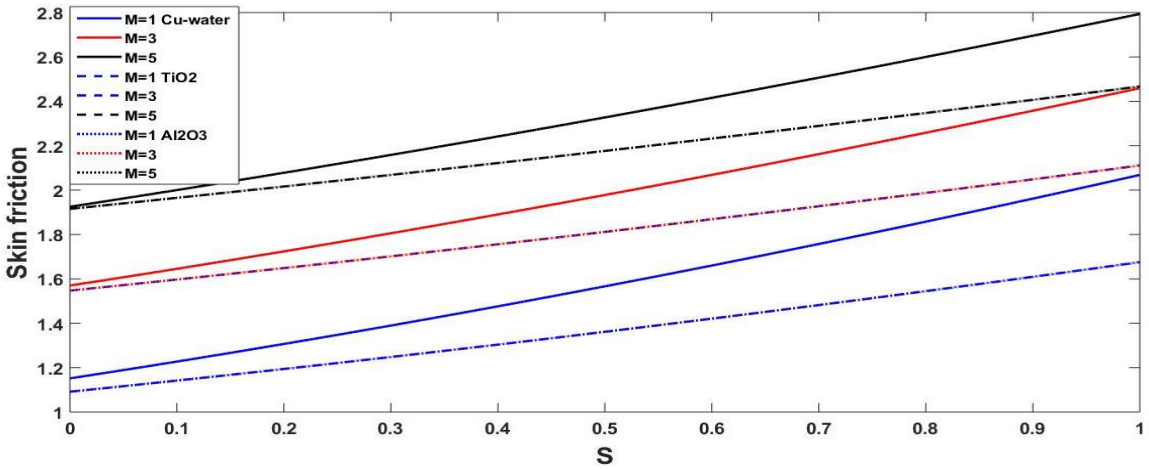

Figure 11: Action of Ha versus S on skin friction

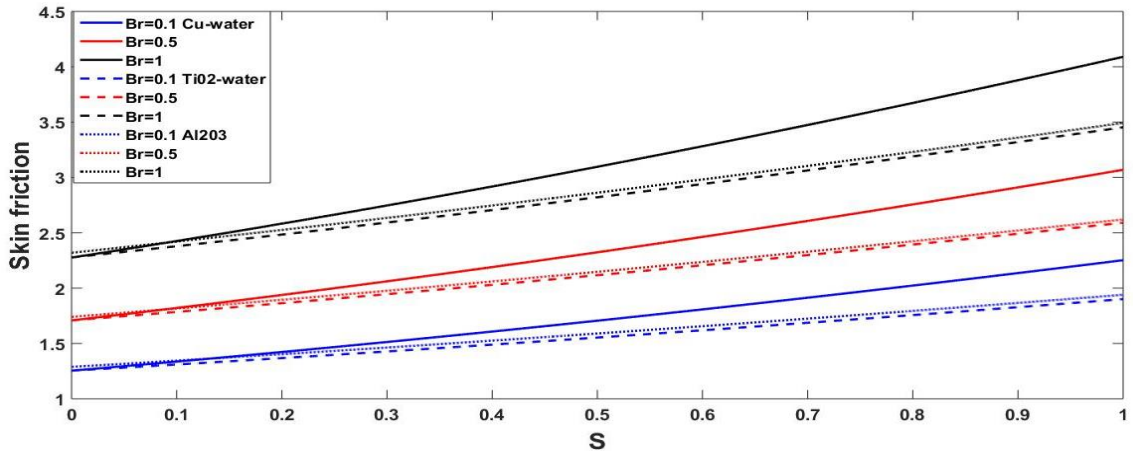

Figure 12: Action of Br against S on Skin friction

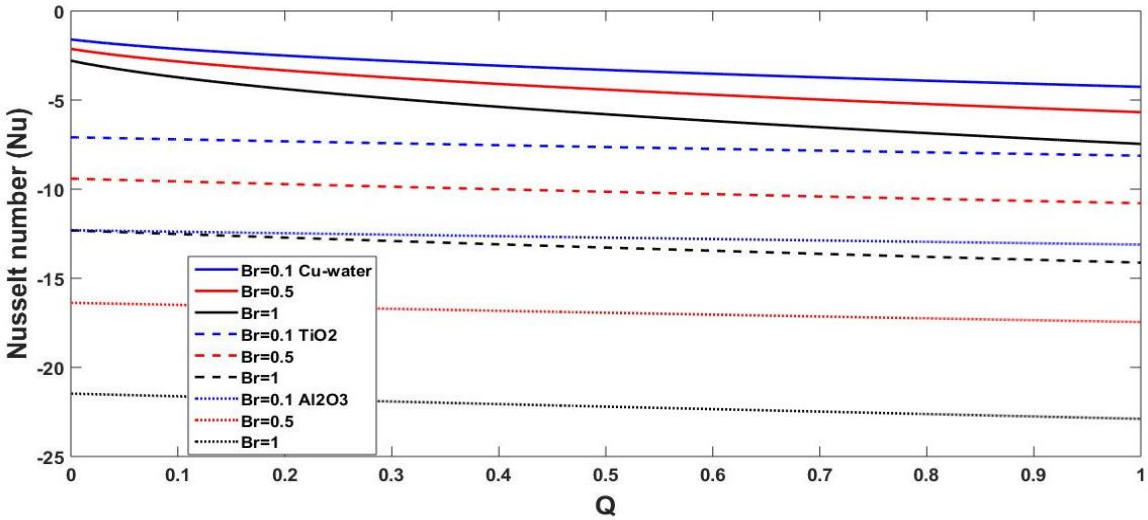

Figure 13: Action of Br against Q on Nusselt number

5.0 CONCLUSION

The impact of Brickman number representing the viscous dissipation on mixed convection magnetized oscillatory flow in a permeable plate equipped with nanoparticles and porous material was examined. The nanofluid velocity, temperature and concentration profiles have been calculated for pertinent controlling parameters on the flow configuration. The physical components of engineering interest have also been computed such as nanofluid skin friction, Nusselt number and Sherwood number. We hope that the findings of this investigation may be useful in catalysis, biomedicine, magnetic resonance imaging, data storage and

environmental remediation. Hence, the subject of nanofluids is of great interest worldwide for basic and applied research. The summary of the noteworthy findings is given below:

i. It is revealed that raising the mixed convection parameter and Brickman number lead to a rise in fluid nanoparticle temperature and velocity respectively.
ii. The copper nanoparticles proved to have the maximum cooling recital for this vertical porous plate problem where Alumina nanoparticles have the lowest. This is due to the high thermal conductivity of Cu and low thermal conductivity of Al_2O_3 and TiO_2
iii. The velocity profile decreases with an increase in nanoparticle magnetic parameter, while the opposite is true when the Darcy porous parameter is increased.
iv. Due to chemical reaction, the concentration of the fluid decreases. This is because the consumption of chemical species leads to a fall in the species concentration field. This remarkable feature of the concentration profiles in our investigation is due to the presence of Soret number and nanoparticles in the flow field.
v. It has been shown that mixing nanoparticles in a liquid (nanofluid) has a dramatic effect on the liquid thermophysical properties such as thermal conductivity.

Conflict of Interest

The authors have declared no conflict of interest.

REFERENCES

Ajibade, A. O. and Umar, A.M. (2016). Effect of chemical reaction and radiation absorption on the unsteady MHD free convection Couette flow in a vertical channel filled with porous materials. *Afrika Matematika*, 27, 201–213.

Ahmad, S. K., Muhammad, H.A., Hamza, M. M., Ojemeri, G. and Usman, U (2024). Magnetized Oscillatory Jeffrey Fluid Flow in A Porous Channel with Unequal Wall Temperature, Dutse Journal of Pure and Applied Sciences (DUJOPAS), 10(2c), 261-272.

Bafakeeh O. T., Raza A., Khan U. S., Khan M. I., Nasr A., Khedher N.B. and Tag-Eldin E.M. (2022). Physical interpretation of Nanofluid (Copper Oxide and Silver) with slip and mixed convection effects: Application of fractional derivatives; Applied Sciences, 12 (21), 10860.

Baoku, I. and Fadare, S.A. (2018). Thermo-diffusion and diffusion -thermo effects on mixed convection hydromagnetic flow in a third-grade fluid over a stretching surface in a Darcy forchheimer porous medium. FUDMA Journal of Sciences, 2(1), pp. 23-42.

Casson, N. (1959). Flow equation for pigment oil suspensions of the printing ink type. Rheology of disperse systems, 84(2), Choi, S.U., Eastman, J. A. Enhancing thermal conductivity of fluids with nanoparticles. No. ANL/MSD/CP-84938: CONF-951135-29.

Choi, S. U. and Eastman, J.A. (1995). Enhancing thermal conductivity of fluids with nanoparticles. (No. ANL/MSD/CP-84938: CONF-951135-29.

Falade, J. A., Ukaegbu, J., Egere, A. C., and Adesanya, S., (2017). MHD Oscillatory Flow Through a Porous Channel Saturated with Porous Medium, Alexandria Eng. J., 56(1), pp. 147–152.

Gbadeyan, J. A., Titiloye, E.O., and Adeosun, A.T. (2020). Effect of variable thermal conductivity and viscosity on Casson nanoflui9d flow with convective heating and velocity slip. Heliyon, 6(1), e03076.

Hamza, M. M. Usman, H. Mustafa A. and Isah B. Y. (2011). Chemical Reaction and Slip Condition Effects on MHD Oscillatory Flow Through a Porous Medium, Research Journal of Mathematic and Statistics, 3(4), pp. 130-135.

Khedher, N. B., Ullah, Z., Mahrous, Y. M., Dhahbi, S., Ahmad, S., Abu-Zinadah, H., and Faqihi, A. A. (2024). Viscous dissipation effect on amplitude and oscillating frequency of heat transfer and electromagnetic waves of magnetic driven fluid flow along the horizontal circular cylinder. Case Studies in Thermal Engineering, 55. https://doi.org/10.1016/j.csite.2024.104142.

Mabood, F., and Usman, H. (2019). Multiple slip effects on MHD thermo-solutal flow in porous media saturated by nanofluid. Mathematical modelling of engineering problems, 6(4), 502-510.

Narayana P.V. S. and Venkateswarlu B. (2016). Heat and mass transfer on mhd nanofluid flow past a vertical porous plate in a rotating system, Frontiers in Heat and Mass Transfer, 7(8), DOI: 10.5098/hmt.7.8.

Omokhuale E., Godwin Ojemeri G., Muhammad A. and Usman H. (2024). Significance of Viscous Dissipation on Hydromagnetic Oscillatory Flow Affected by Nanoparticles Through a Boundary Layer Regime, International Journal of Development Mathematics, 1(2), 098 - 113 .

Raghunath, K. and Obulesu, M. (2022). Unsteady MHD oscillatory Casson fluid flow past an inclined vertical porous plate in the presence of chemical reaction with heat absorption and Soret effects. Heat Transfer, 51, 733–752.

Raghunath, K., Nagesh, G., Reddy, V.R.C. and Obulesu, M. (2021). Unsteady MHD fluid flow past an inclined vertical porous plate in the presence of chemical reaction with aligned magnetic field, radiation, and Soret effects. Heat Transfer,51,2742–2760.

Raghunath, K., Obulesu, M., Sujatha, S. and Venkateswaraju, K. (2022). Investigation of MHD

Casson fluid flow past a vertical porous plate under the influence of thermal diffusion and chemical reaction. Heat Transfer, 51, 377–394.

Reddy, V. R., Raghunath, K. and Obulesu, M. (2022). Characteristics of MHD Casson fluid past an inclined vertical porous plate. Material Today for Proceses., 49, 2136–2142.

Saleem, S., Nazeer, M., Radwan, N., and Abutuqayqah, H. (2024). Significance of hafnium nanoparticles in hydromagnetic non-Newtonian fluid-particle suspension model through divergent channel with uniform heat source: thermal analysis. Zeitschrift für Naturforschung A, (0). https://doi.org/10.1515/zna-2023-0336

Salah F., Sidahmed A. O. M. and Viswanathan K. K. (2023). Chemical MHD Hiemenz flow over a nonlinear stretching sheet and Brownian motion effects of nanoparticles through a porous medium with radiation effect, Mathematical Computer and Modeling of Fluid Flow and Heat Transfer, 28(1), 21, DOI: 10.3390/mca28010021 .

Sharma T., Sharma P. and Kumar N. (2022). Study of dissipative MHD oscillatory unsteady free convective flow in a vertical channel occupied with the porous material in the presence of heat source effect and thermal radiation, International Symposium on Fluids and Thermal Engineering, 012012. doi:10.1088/1742-6596/2178/1/012012.

Usman H., Muhammad A. and Omokhuale E. (2024). Enhancing thermophoresis effect on time-dependent magnetohydrodynamics (MHD) oscillatory boundary layer flow occupied with nanoparticles, International Journal of Science for global sustainability, 10(1), 197-207. https://doi.org/10.57233/ijsgs.v10i1.611

Usman and Sanusi (2023). Heat and mass transfer analysis for the mhd flow of Casson nanofluid in the presence of thermal radiation, FUDMA Journal of Sciences, 7(2), pp 188 – 198.

Appendix

$c_1 = c_3 = c_5 = c_7 = \frac{-A_5SPr+\sqrt{(A_5SPr)^2+4A_2Q}}{2A_2}$, $c_2 = c_4 = c_6 = c_8 = \frac{A_5SPr+\sqrt{(A_5SPr)^2+4A_2Q}}{2A_2}$,
$c_9 = c_{11} = c_{13} = c_{15} = \frac{-SSc+\sqrt{(SSc)^2+4ScKr}}{2}$, $c_{10} = c_{12} = c_{14} = c_{16} = \frac{SSc+\sqrt{(SSc)^2+4ScKr}}{2}$,
$c_{17} = c_{19} = c_{21} = c_{23} = \frac{-A_1A_3S+\sqrt{(A_1A_3S)^2+4A_1w_2}}{2}$, $c_{18} = c_{20} = c_{22} = c_{24} = \frac{A_1A_3S+\sqrt{(A_1A_3S)^2+4A_1w_2}}{2}$,
$w_2 = A_3iR + Ha + \frac{1}{Da}, H_5 = \frac{-Prc_{18}^2D_2^2}{4A_2c_{18}^2-2A_5SPrc_{18}-Q}, H_6 = \frac{-2Prc_2c_{18}D_2D_3}{A_2(-c_{18}-c_2)^2-A_5SPr(-c_{18}-c_2)-Q}, H_7 = \frac{-Prc_2^2D_3^2}{4A_2c_2^2-2A_5SPrc_2-Q}, H_4 = 1 - H_5 - H_6 - H_7,\ F_{10} = \frac{-Prc_{20}^2D_{10}^2}{4A_2c_{20}^2-2A_5SPrc_{20}-Q},\ H_{11} = \frac{-2Prc_6c_{20}D_{10}D_{11}}{A_2(-c_{20}-c_6)^2-A_5SPr(-c_{20}-c_6)-Q}, H_{12} = \frac{-Prc_6^2D_{11}^2}{4A_2c_6^2-2A_5SPrc_6-Q}, H_9 = 1 - H_{10} - H_{11} - H_{12}, L_3 = \frac{-ScSrc_2^2}{4c_2^2-SSc c_2-ScKr},\ L_2 = 1 - L_3, L_6 = \frac{-ScSrc_4^2F_4}{c_4^2-SSc c_4-ScKr}, L_7 = \frac{-4ScSrc_{18}^2F_5}{4c_{18}^2-2SSc c_{18}-ScKr}, L_8 = \frac{-ScSr(-c_{18}-c_2)F_6}{(-c_{18}-c_2)^2-SSc(-c_{18}-c_2)-ScKr}, L_9 = \frac{-4ScSrc_2^2F_7}{4c_2^2-2SSc c_2-ScKr}, L_5 = 1 - L_6 - L_7 - L_8 - L_9,$
$L_{11} = 1 - L_{12}, \square_{15} = \frac{-ScSrc_8^2F_9}{c_8^2-SSc c_8-ScKr}, \square_{16} = \frac{-4ScSrc_{20}^2F_{10}}{4c_{20}^2-2SSc c_{20}-ScKr},\ L_{17} = \frac{-4ScSr(-c_{20}-c_6)^2F_{11}}{4(-c_{20}-c_6)^2-SSc(-c_{20}-c_6)-ScKr}, L_{18} = \frac{-4ScSrc_6^2F_{12}}{4c_6^2-2SSc c_6-ScKr}, L_{14} = 1 - L_{15} - L_{16} - L_{17} - L_{18},\ E_3 = \frac{-A_4}{\frac{c_2^2}{A_1}-A_3Sc_2-w_2}\ E_2 = 1 - E_3,\ E_6 = \frac{-A_4F_4}{\frac{c_4^2}{A_1}-A_3Sc_4-w_2},\ E_7 = \frac{-A_4F_5}{\frac{c_{18}^2}{A_1}-A_3Sc_{18}-w_2},\ E_8 = \frac{-A_4F_6}{\frac{(-c_{18}-c_2)^2}{A_1}-A_3S(-c_{18}-c_2)-w_2}, E_9 = \frac{-A_4H_7}{\frac{c_2^2}{A_1}-2A_3Sc_2-w_2}, E_5 = 1 - E_6 - E_7 - E_8 - E_9,$
$E_{10} = \frac{-A_4}{\frac{c_6^2}{A_1}-A_3Sc_6-w_2},\ E_9 = 1 - E_{10},\ E_{13} = \frac{-A_4}{4\frac{c_6^2}{A_1}-2A_3Sc_6-w_2},\ E_{12} = 1 - E_{13},$
$E_{15} = \frac{-A_4H_9}{\frac{c_8^2}{A_1}-A_3Sc_8-w_2},\ E_{16} = \frac{-A_4H_{10}}{\frac{4c_{20}}{A_1}-2A_3Sc_{20}-w_2},\ E_{17} = \frac{-A_4H_{11}}{\frac{(-c_{20}-c_6)^2}{A_1}-A_3S(-c_{20}-c_6)-w_2},\ E_{18} =$

DOI: https://doi.org/10.57233/ijsgs.v10i2.672 ISSNp: 2488-9229; ISSNe: 3027-1118
IJSGS FUGUSAU VOL10 (2) WEBSITE: https://fugus-

$\frac{-A_4 H_{12}}{\frac{4c_6^2}{A_1}-2A_3 Sc_6-w_2}$, $E_{14} = 1 - E_{15} - E_{16} - E_{17} - E_{18}$,

Nomenclature

B_0 constant applied magnetic field
τ skin friction coefficient
C_p specific heat at constant pressure
C_∞ concentration of the solute far away from the plate
D_m molecular diffusivity
E applied electric field
g acceleration due to gravity
Da Darcy porous parameter
k permeability of porous medium
k∗ mean absorption coefficient
Ha dimensionless magnetic field parameter
Nu Nusselt number
Pr Prandtl number
Br Brickman number
Q dimensional heat sink parameter
R dimensional rotational parameter
Kr chemical reaction parameter
S suction parameter
Sc Schmidt number
Sr Soret number
$\frac{Gr}{Re} = Gre$ Mixed convection parameter
γ constant pressure gradient
Sh Sherwood number
w condition at the wall
T local Temperature of the Nano fluid
T_w wall temperature of the fluid
T_∞ temperature of the ambient Nano fluid
U_0 characteristic velocity
(u,v,w) velocity components along x and y axes

Greek Symbols

α thermal diffusivity
α_f thermal diffusivity of the fluid
α_{nf} thermal diffusivity of the nanofluid
β thermal expansion coefficient
β_f coefficient of thermal expansion of the fluid
β_s coefficient of thermal expansion of the solid
$(\rho C_p)_{nf}$ heat capacitance of the nanofluid
σ ∗ Stefan-Boltzmann constant parameter
σ electrical conductivity of the fluid
ρ_f density of the fluid friction
ρ_{nf} density of the nanofluid
ρ_s density of the solid friction
v_f kinematic viscosity of the fluid
ν kinematic viscosity
μ_{nf} viscosity of the nanofluid
μ dynamic viscosity
ε small constant quantity
U complex velocity
T non-dimensional Temperature
C non-dimensional Concentration

Subscript

f fluid
s solid
n_f Nano fluid
∞ Condition at free stream